Evidence for a Quasi-Two-Dimensional Proton Glass State in $Cs_5H_3(SO_4)_4 \cdot xH_2O$ Crystals

S. G. Lushnikov, S. N. Gvasaliya, and A. I. Fedoseev
A.F. Ioffe Physical Technical Institute RAS, 194021 St. Petersburg, Russia

V. H. Schmidt and G. F. Tuthill
Physics Department, Montana State University, Bozeman, Montana 59717

L. A. Shuvalov
Institute of Crystallography RAS, 117333 Moscow, Russia
(Received 26 May 2000)

We describe damping of hypersonic and ultrasonic longitudinal acoustic (LA) phonons in crystals of $Cs_5H_3(SO_4)_4 \cdot xH_2O$ (PCHS) between 100 and 360 K. The damping of LA phonons exhibits strong dispersion caused by relaxation processes in the region of transformation into the glasslike phase ($T_g \approx$ 260 K). Near T_g the damping of ultrasonic phonons propagating in the basal plane reflects the cooperative freezing of acid protons. The damping of LA phonons propagating perpendicular to the basal plane can be fit by the Debye model and is due to the interaction between protons and LA phonons. This suggests that the proton glass state that is realized at $T < T_g$ has a quasi-two-dimensional nature.

DOI: 10.1103/PhysRevLett.86.2838 PACS numbers: 63.20.–e, 64.60.Ht, 64.70.Pf, 78.35.+c

Crystals of $Cs_5H_3(SO_4)_4 \cdot xH_2O$ (PCHS) belong to a new class of compounds with the common formula $M_zH_y(AO_4)_{(z+y)/2} \cdot xH_2O$, where $M = Cs, Rb, NH_4$; $A = S, Se$; $0 \leq x \leq 1$ [1]. The high-temperature phase of these crystals has a dynamically disordered network of hydrogen bonds responsible for the high protonic conductivity referred to as superprotonic [2,3]. Protons play a decisive role in the lattice dynamics of these compounds. A strong hydrogen isotope effect in some materials of the type of $MHAO_4$, $M_3H(AO_4)_2$, and $M_5H_3(AO_4) \cdot nH_2O$ manifests itself as additional phases and structural phase transitions [4–6]. The protonic conductivity of PCHS is quasi-two-dimensional, $\sigma_a/\sigma_c \sim 50$, so conductivity in the basal plane is nearly 2 orders of magnitude higher than along the hexagonal axis [1]. This reflects a feature of the PCHS crystal structure, that layers of SO_4 tetrahedra linked by hydrogen bonds are located in the basal plane. In this quasi-two-dimensional dynamic network of hydrogen bonds, the number of structurally equivalent positions for protons is 3 times as large as the number of protons.

At room temperature, the PCHS crystals belong to the hexagonal system with space group $P6_3/mmc$ ($a = 6.2455$ Å, $c = 29.690$ Å; $V = 1003$ Å^3; $Z = 2$) [7]. Events of particular interest occur in the vicinity of $T_{c1} = 414$ K and $T_{c2} = 360$ K. At T_{c1}, a superprotonic phase transition is accompanied by a symmetry change $P6/mmm \Leftrightarrow P6_3/mmc$ [7,8], and at T_{c2} an isostructural phase transition takes place, associated with changes in the local symmetry of SO_4 tetrahedra [9–11]. No other anomalies associated with structural changes in protonic samples were observed. As the temperature decreases, the dynamic disorder of the hydrogen bond network gives way to static disorder (both orientational and positional), and in the vicinity of $T_g = 260$ K a transformation into a proton-glass-like phase occurs [12]. These features make PCHS crystals unique objects for studies of the effect of disorder on physical properties.

The goal of this work was to study the damping of longitudinal acoustic phonons at different frequencies by using the results of our Brillouin experiments and comparing them with the ultrasonic data given in [13].

Colorless single crystals of PCHS were grown by slow evaporation from a saturated water solution at room temperature. The samples were plates with a developed basal plane and typical hexagonal facets. The crystal orientation was determined by using a polarizing microscope. For each temperature cycle a separate sample was used, and, hence, all single crystals used in our experiments had identical prehistory.

Light scattering spectra were excited by a single-mode Ar^+ Spectra-Physics laser with $\lambda = 488$ nm. A backscattering geometry was used. The scattered light was analyzed by a three-pass piezoscanning Fabry-Perot interferometer with a Burleigh DAS-1 system with automatic signal acquisition and automatic alignment of the interferometer mirrors. This provided a finesse of the interferometer of $C = 50$. During the measurements, the free spectral range of the interferometer varied between 11 and 14 GHz.

The velocity (V) and damping (α) of longitudinal hypersonic phonons in the 180° scattering geometry were determined by the relations

$$V = \nu\lambda/2n, \tag{1}$$

$$\alpha = 4\pi n\delta/v\lambda, \tag{2}$$

where n is the refractive index of the crystal, ν is the shift of the Brillouin component, and δ is its half width at half maximum. In all calculations, we used $n = 151$ [14]. In

 0031-9007/01/86(13)/2838(4)$15.00

this work, the temperature behavior of longitudinal hypersonic phonons (LA) with $\mathbf{q}_{ph} \parallel \mathbf{c}_h$ and $\mathbf{q}_{ph} \perp \mathbf{c}_h$ ($\mathbf{q}_{ph}$ is the acoustic phonon wave vector) in the PCHS crystals was studied. The LA phonon velocity in a hexagonal crystal is determined by the elastic moduli $C_{33} = \rho V^2$ for $\mathbf{q}_{ph} \parallel \mathbf{c}_h$ and by $C_{11} = \rho V^2$ for $\mathbf{q}_{ph} \perp \mathbf{c}_h$, where ρ is the crystal density whose value was taken from Ref. [7].

Figure 1 shows, in the range 120 to 360 K, the damping of hypersonic LA phonons with wave vector $\mathbf{q}_{ph}$ either directed along the C_6 axis or lying in the basal plane. The hypersonic phonon damping is independent of direction at low temperature, increasing steadily with temperature and exhibiting no anomaly in the vicinity of T_g. Above 300 K, the damping increases more rapidly, and begins to depend markedly on direction. A pronounced increase in damping of basal plane phonons sets in near 320 K, while the onset of similar behavior for the phonons with $\mathbf{q}_{ph} \parallel C_6$ does not occur until 350 K. Above 360 K, we could not detect the Brillouin component in the light scattering spectra. A similar behavior was observed in Raman scattering experiments, where the background and quasielastic scattering contribution increased sharply in the vicinity of $T = 360$ K [9], indicating significant changes in the light scattering conditions in the crystal (formation of cracks, inhomogeneities, etc.). In Ref. [11], hypersonic damping anomalies near 360 K were attributed to an isostructural phase transition.

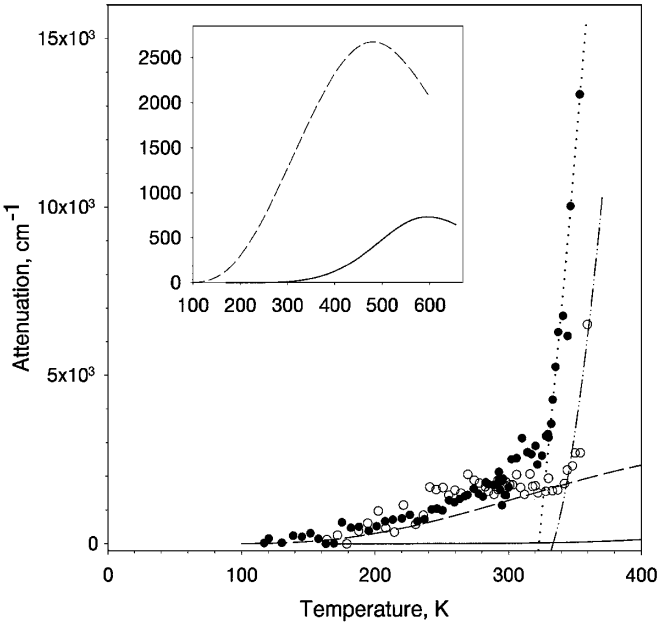

FIG. 1. Temperature dependences of the damping of the longitudinal hypersonic acoustic phonons of PCHS crystals. Solid circles show experimental data for the phonons with $\mathbf{q}_{ph} \perp \mathbf{c}_h$. Open circles show experimental data for the phonons with $\mathbf{q}_{ph} \parallel \mathbf{c}_h$. The solid line shows changes in the damping of LA phonons with $\mathbf{q}_{ph} \parallel \mathbf{c}_h$ at hypersonic frequencies recalculated from ultrasonic data using Eq. (3). The dashed line shows changes in the damping of LA phonons with $\mathbf{q}_{ph} \perp \mathbf{c}_h$ at hypersonic frequencies recalculated from ultrasonic data using Eq. (6). The inset presents the hypothetical behavior of the relaxational damping of the hypersonic LA phonons in a wide temperature range. The meanings of the lines are the same as in the main figure.

Our Brillouin data show that the anomalously large damping of hypersonic LA phonons is strongly anisotropic. The difficulty of extracting the Brillouin component at high temperatures, plus the fact that near 430 K the PCHS crystal begins to decompose, prevented us from further analyzing the damping in this intriguing region. For this reason, we reanalyzed the ultrasound data of Ref. [13], where the damping anomaly—a broad maximum correlated with a velocity shift—occurs over a lower, accessible temperature range, and allows us to test several alternative models.

Relaxation of acoustic phonons is described by several approaches. The simplest is the Debye model, which is appropriate to identical independent subsystems characterized by a single relaxation time τ. The attenuation α in this case is

$$\alpha = \frac{NB^2}{4\pi\rho\nu^3 k_B T}\,\omega\,\frac{\omega\tau}{1 + \omega^2\tau^2}, \tag{3}$$

where N is the concentration of mobile ions, B is the deformation potential constant, and k_B is the Boltzmann constant. The temperature dependence of the relaxation time is assumed to take the form $\tau = \tau_0 \exp(E_a/k_B T)$.

However, there are many situations where the relaxation damping curve is much broader than the Debye one, which means that the attenuation cannot be described in terms of one relaxation time. A common approach then involves a model with a distribution of relaxation times, so that the damping can be the sum of several Debye peaks. Each Debye-type "relaxator" interacts independently with the deformation field. This approach has been applied to a large number of compounds [15–19]. The attenuation is then

$$\alpha = \frac{NB^2}{4\pi\rho\nu^3 k_B T}\,\omega\int dE\,\frac{g(E)\omega\tau(E)}{1 + \omega^2\tau(E)^2}, \tag{4}$$

where $g(E)$ corresponds to a distribution of activation energies, often taken to be Gaussian with mean E_a and width E_0:

$$g(E) = \frac{1}{E_0\sqrt{2\pi}}\exp\left\{-\frac{(E - E_a)^2}{2E_0^2}\right\}. \tag{5}$$

In certain materials, the assumption of independent relaxators cannot be justified. This is the case in superionic conductors [20], where the concentration of mobile ions is fairly high. In such situations, the relaxing system will exhibit pronounced cooperative behavior, and the attenuation is best described [16,19,21] by the so-called universal model,

$$\alpha \propto \frac{1}{T}\,\omega\,\frac{(\omega\tau)^m}{1 + (\omega\tau)^{1+m-n}}, \tag{6}$$

where $0 \le m, n \le 1$. Here the damping maximum is reached when the condition $\omega\tau = [m/(1 - n)]^{1/(1-n+m)}$ is satisfied. The Debye model corresponds to the special

case $m = 1$ and $n = 0$ of the universal model, as well as to the special case $g(E) = \delta(E - E_a)$ of the model with the distribution of relaxation times.

We next examine the ultrasound attenuation data of Ref. [13] in light of the above models. In Fig. 2(a), we display the data for phonons with $\mathbf{q}_{ph} \parallel C_6$, together with a solid line showing the best fit to the Debye model with $\tau_0 = 4.8 \times 10^{-14}$ s, $E_a = 0.28$ eV. These parameters correspond well to the attempt time and barrier energy of protons in the double-minimum potential of the hydrogen bond. The fit is excellent over the temperature range of the anomaly, with standard deviation 0.04. The authors of Ref. [13] attempted a fit with a distribution of activation energies, and found a very small dispersion ($E_0 = 0.008$ eV, $E_0/E_a \sim 0.03$), corresponding nearly to a delta function. The simple Debye model is sufficient to describe attenuation of LA phonons propagating along the C_6 axis. Damping in this case is governed by the interaction of acoustic waves with the individual protons in the hydrogen bonds.

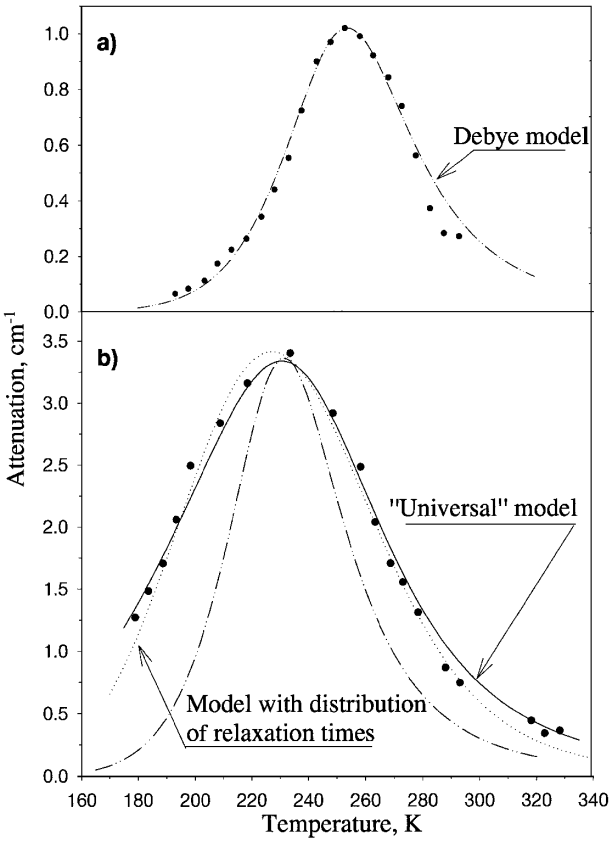

FIG. 2. (a) Damping of ultrasonic LA phonons with $\mathbf{q}_{ph} \parallel \mathbf{c}_h$. Solid circles show experimental data taken from Ref. [13]. The solid line indicates our calculation in the framework of the classical Debye model using Eq. (3). (b) Damping of ultrasonic LA phonons with $\mathbf{q}_{ph} \perp \mathbf{c}_h$. Solid circles show experimental data taken from Ref. [13]. The dash-and-dotted line indicates our calculation in the framework of the Debye model using Eq. (3). Dots show calculation using the model with a distribution of activation energies [Eq. (4)]. The solid line is our calculation using the universal model [Eq. (5)].

Figure 2(b) shows the temperature-dependent attenuation of ultrasonic phonons propagating in the basal plane in PCHS. The Debye model (dash-dotted line, with best fit parameters $\tau_0 = 1.5 \times 10^{-15}$ s, $E_a = 0.255$ eV) is clearly inadequate. A Gaussian distribution of activation energies allows us to achieve a good fit, as shown by the dotted line. However, the parameters $\tau_0 = 1.5 \times 10^{-15}$ s, $E_a = 0.32$ eV, and $E_0 = 0.057$ are not physically meaningful; the relaxation time is too low and the dispersion of energies rather large. To achieve consistency between model and experiment, the integral of Eq. (4) had to be carried out over an interval of $6E_0$; the physical reason for such a wide range of activation energies for individual relaxators is unclear.

Only the fit to the universal model gave excellent agreement (solid line, standard deviation equal to 0.14), with $m = 0.85$, $n = 0.65$, and values for the fundamental relaxation time and activation energy ($\tau_0 = 4.8 \times 10^{-14}$ s, $E_a = 0.27$ eV) that are physically reasonable. Note that these values of τ_0 and E_a agree with those found by fitting the C_6 ultrasonic phonon data to the Debye model. This demonstrates that we properly chose the models, because it is reasonable that the parameters of the double-minimum potential do not depend on the crystallographic direction. Moreover, with these m and n, the attenuation maximum of the universal model, given by the condition $\omega\tau = [m/(1 - n)]^{1/(1-n+m)}$, should be shifted downward in temperature to about 0.94 that of the Debye model with the same E_a and τ_0. Comparing Figs. 2(a) and 2(b), we see that the ratio of temperature maxima is approximately 0.92. This further supports our use of these two models to describe attenuation of phonons propagating within and perpendicular to the basal plane. Thus, in the basal plane where the number of protons in energetically equivalent positions is much larger than in the hexagonal axis direction, damping is governed by a collective behavior of the proton system.

As a test of the models, we use the values for E_a, τ_0, m, and n, obtained by fitting the ultrasonic data, to calculate the attenuation of hypersonic LA phonons. The solid and dashed lines of Figs. 1 illustrate the result, compared with our actual Brillouin data. Near T_g, the calculated attenuation at hypersonic frequencies agrees with experiment but, above room temperature, the hypersonic damping departs dramatically from the model. We observe a sharp growth of damping for $T > 320$ K, while in the models the increase is far more gradual. Acoustic response anomalies near an isostructural phase transition T_{c2} [16] may cause the additional damping near 360 K. The models do predict (see the inset of Fig. 1) attenuation maxima at hypersonic frequencies, but at temperatures well above that at which the crystal becomes unstable.

It is useful to compare τ_0 and E_a that we find from fitting the data of Ref. [13], with values based on other measurements on PCHS. Fits obtained from NMR [22] give a substantially larger (0.34 eV) activation energy and a time constant τ_0 twenty times larger than our result,

possibly because these numbers represent averaged estimates from measurements on powder samples. Dielectric studies [12,23] give very similar values for the activation energy, and time constants in the same general range.

We have shown that the mechanism of LA phonon damping at ultrasonic frequency near T_g depends strongly on the crystallographic direction. For an ultrasonic acoustic phonon propagating along the hexagonal axis, damping is described by the Debye model, whereas for ultrasonic phonons propagating in the basal plane the anomaly near T_g is best fit by the universal model involving cooperative proton behavior. This situation, where relaxation is governed by individual identical Debye relaxators in one direction and by cooperative behavior of relaxators in another direction, is unusual; to our knowledge, no analogous situation has been described. The contrasting behaviors can be explained if we suppose that below T_g a quasi-two-dimensional proton glass state is present. This means that the processes in the lattice dynamics of PCHS associated with "freezing" are pronounced in the basal plane and are negligibly weak along the hexagonal axis. This suggested picture corresponds to structural features of the PCHS crystal: the quasi-two-dimensionality of the dynamically disordered network of hydrogen bonds is preserved at and below the freezing temperature. These processes are also reflected in the anisotropy of the α relaxation revealed in the analysis of the dielectric response dispersion [13]. We suppose that the key role in the lattice dynamics is played by dipoles formed by random orientation of complexes consisting of SO_4 groups and protons connecting them in the basal plane. In accord with this supposition, we have obtained evidence that the proton glass state in the PCHS crystal can be defined as a quasi-two-dimensional system, or quasi-two-dimensional proton glass.

In summary, we have carried out studies of the behavior of longitudinal acoustic phonons in PCHS over a wide temperature range, including the region of transformation into the glasslike state. Analysis of acoustic properties at hypersonic ($f \sim 17$ GHz) and ultrasonic ($f \sim 10$ MHz, from Ref. [13]) frequencies reveals an unusual anisotropy in the phonon damping near the glass transition at the lower (ultrasonic) frequency. The temperature dependence of the damping also changes drastically with frequency, with a well-defined damping maximum present in the ultrasonic data near T_g, but absent at hypersonic frequency. Comparison of the measured ultrasonic attenuation with common phenomenological models suggests the most probable mechanisms of mechanical relaxation in the main directions, along the sixfold axis and in the basal plane. Propagation of longitudinal acoustic phonons along the C_6 axis can be described by the Debye model, while for phonons propagating in the basal plane the damping appears to be governed by the collective behavior of protons located in energetically equivalent positions on hydrogen bonds. We conclude that the proton glass state in PCHS at $T \leq 260$ K has a quasi-two-dimensional character. Numerical simulations may be a practical and interesting approach to modeling the glass state qualitatively and quantitatively.

The authors thank V. V. Dolbinina for growing samples. The work was supported by Russian Foundation for Basic Research, Grant No. 99-02-18356, and National Science Foundation, Grant No. DMR-9805272.

[1] A. I. Baranov, O. A. Kabanov, B. V. Merinov, L. A. Shuvalov, and V. V. Dolbinina, Ferroelectrics **127**, 257 (1992).
[2] B. V. Merinov, A. I. Baranov, L. A. Shuvalov, and B. A. Maksimov, Kristallografiya **32**, 86 (1987) [Sov. Phys. Crystallogr. **32**, 111 (1987)].
[3] D. Abramic, J. Dolinšek, R. Blinc, and L. A. Shuvalov, Phys. Rev. B **42**, 442 (1990).
[4] T. Fukami and R. H. Chen, Phys. Status Solidi (b) **214**, 219 (1999).
[5] M. Sumita, T. Osaka, and Y. Makita, J. Phys. Soc. Jpn. **51**, 1343 (1982).
[6] S. G. Lushnikov, A. V. Belushkin, S. N. Gvasaliya, I. Natkaniec, L. A. Shuvalov, L. S. Smirnov, and V. V. Dolbinina, Physica (Amsterdam) **276B–278B**, 483 (2000).
[7] B. V. Merinov, A. I. Baranov, L. A. Shuvalov, J. Schneider, and H. Schulz, Solid State Ion. **74**, 53 (1994).
[8] Yu. I. Yuzyuk, V. P. Dmitriev, V. V. Loshkarev, L. M. Rabkin, and L. A. Shuvalov, Ferroelectrics **167**, 53 (1995).
[9] Yu. I. Yuzyuk, V. P. Dmitriev, V. V. Loshkarev, L. M. Rabkin, and L. A. Shuvalov, Kristallografiya **39**, 70 (1994) [Crystallogr. Rep. **39**, 61 (1994)].
[10] S. G. Lushnikov and L. A. Shuvalov, Kristallografiya **44**, 662 (1999) [Crystallogr. Rep. **44**, 615 (1999)].
[11] S. G. Lushnikov, V. H. Schmidt, L. A. Shuvalov, and V. V. Dolbinina, Solid State Commun. **113**, 639 (2000).
[12] A. I. Baranov, O. A. Kabanov, and L. A. Shuvalov, Pis'ma Zh. Eksp. Teor. Fiz. **58**, 542 (1993) [JETP Lett. **58**, 548 (1993)].
[13] E. D. Yakushkin and A. I. Baranov, Fiz. Tverd. Tela (Leningrad) **39**, 89 (1997) [Sov. Phys. Solid State **39**, 77 (1997).
[14] F. Kadlec, Yu. Yuzyuk, P. Simon, M. Pavel, K. Lapsa, P. Vanek, and J. Petzelt, Ferroelectrics **176**, 179 (1996).
[15] P. Esquinazi and R. Koning, in *Tunneling Systems in Amorphous and Crystalline Solids,* edited by P. Esquinazi (Springer-Verlag, New York, 1998).
[16] D. P. Almond and A. R. West, Solid State Ion. **26**, 265 (1988).
[17] J. Jackle, L. Piche, W. Arnold, and S. Hunklinger, J. Non-Cryst. Solids **20**, 365 (1976).
[18] L. Börjesson, Phys. Rev. B **36**, 4600 (1987).
[19] D. P. Almond and A. R. West, Phys. Rev. Lett. **47**, 431 (1981).
[20] J. B. Boyce and B. A. Huberman, Phys. Rep. **51**, 191 (1979).
[21] A. K. Jonscher, Nature (London) **267**, 673 (1977).
[22] A. M. Fajdiga-Bulat, G. Lahajnar, J. Dolinšek, J. Slak, B. Lozar, B. Zalar, L. A. Shuvalov, and R. Blinc, Solid State Ion. **77**, 101 (1995).
[23] Yu. Yuzyuk, V. Dmitriev, L. Rabkin, L. Burmistrova, L. Shuvalov, F. Smutny, P. Vanek, I. Gregora, and J. Petzelt, Solid State Ion. **77**, 122 (1995).